Received: 28 April 2020 | Revised: 21 July 2020 | Accepted: 5 October 2020

DOI: 10.1002/aoc.6076

FULL PAPER

Applied Organometallic Chemistry WILEY

Dye-sensitized solar cells based on zinc(II) phthalocyanines bearing 3-pyridin-3-ylpropoxy anchoring groups

Turgut Keleş[1] | **Zekeriya Biyiklioglu**[2] | **Emre Güzel**[3] | **Mehmet Nebioğlu**[4,5] | **İlkay Şişman**[4,5]

[1]Central Research Laboratory Application and Research Center, Recep Tayyip Erdogan University, Rize, Turkey

[2]Department of Chemistry, Karadeniz Technical University, Trabzon, 61080, Turkey

[3]Department of Fundamental Sciences, Sakarya University of Applied Sciences, Sakarya, Turkey

[4]Department of Renewable Energy Systems, Sakarya University, Sakarya, 54050, Turkey

[5]Department of Chemistry, Sakarya University, Sakarya, 54050, Turkey

Correspondence
Zekeriya Biyiklioglu, Department of Chemistry, Karadeniz Technical University, 61080 Trabzon, Turkey.
Email: zekeriyab@ktu.edu.tr

In this study, nonperipherally tetra-substituted (**2**), peripherally tetra-substituted (**3**), and peripherally octa-substituted (**4**) zinc(II) phthalocyanines were synthesized as sensitizers for dye-sensitized solar cells (DSSCs) in which 3-pyridin-3-ylpropoxy substituent acts as anchoring unit to bind TiO_2 surface. The optical results indicated that there is an interaction between the dyes and the TiO_2 surface. The photovoltaic performances of the DSSCs based on these dyes were found to depend on both the position and number of the substituents. Despite the more red-shifted absorption, the DSSC based on **2** showed the conversion efficiency of 0.68%, which is lower than 1.36% and 0.92% for **3** and **4**, respectively, under one sun (AM 1.5G). The vertical orientation of the dye on TiO_2 surface could be the main reason for the higher photovoltaic performance of complex **3**, which is beneficial for not only injecting the electrons into the conduction band of TiO_2 but also reducing the charge recombination. Overall, these results demonstrate that the peripherally tetra-substituted 3-pyridin-3-ylpropoxy zinc(II) phthalocyanine complex (**3**) as a sensitizer can more efficiently utilize the photons in the red/near-infrared region with respect to the other complexes studied.

KEYWORDS

3-pyridin-3-ylpropoxy, anchoring group, dye-sensitized solar cells, phthalocyanine

1 | INTRODUCTION

The use of sunlight to produce energy with photovoltaic devices can be considered one of the better alternatives to conventional energy sources. In recent years, dye-sensitized solar cells (DSSCs) have attracted great attention owing to their low production costs and the use of nontoxic materials.[1] DSSCs are new photovoltaic devices formed using wide band gap semiconducting metal oxides including TiO_2, ZnO, and SnO_2 as the electron-transporting materials coated with an organic dye. Among them, TiO_2 has higher conduction band (CB), electron affinity, dye loading, and surface area with respect to other metal oxides, which make it the most popular electron-transporting electrode for DSSCs.[2] The organic dye acts as an antenna that uses solar radiation to excite and inject into the CB of the TiO_2. In this context, DSSCs using ruthenium complexes as dyes yielded 11.5% power conversion efficiency (PCE) under AM 1.5 irradiation. However, the low absorption coefficient of these ruthenium sensitizers in the red region and the low availability of ruthenium has led to the development of effective and ruthenium-free sensitizers for DSSCs. In contrast to ruthenium dyes, phthalocyanine (Pc) dyes, which are sensitizers with extended π-conjugation, have attracted attention owing to efficient photo-induced electron transfer and high absorption coefficients in the red region of the solar spectrum. These dyes exhibited high

performance in DSSC applications with light-harvesting efficiency up to 700 nm and good thermal and photochemical stability.[3] This makes them attractive for DSSCs. Also, the central metal ion of the phthalocyanines greatly effects their optical, photophysical, electrochemical, and photovoltaic properties.[4,5] In particular, phthalocyanines containing zinc metal ion have been widely studied for DSSC applications owing to both their diamagnetic character[6] and their long-lived (>1 ns) singlet excited states.[1,7] The anchoring groups in DSSCs, such as carboxylic acid, cyanoacrylic acid, or rodanin-3-acetic acid, which generally serve as electron acceptors, are used to ensure that the dye attaches to the TiO_2 surface.[8] The carboxylic acid groups form a strong ester linkage with the TiO_2 surface, providing a strong electronic communication between the dye and the TiO_2 surface. However, using different functional groups as an anchor and electron acceptor can enable the development of new dyes for DSSCs. In order to prepare new and efficient phthalocyanine dyes in DSSCs, different dyes with a stronger interaction between the electron accepting moiety of the sensitizers and the TiO_2 surface can be designed. In this manner, we have prepared three zinc phthalocyanines and evaluated the substituent orientation and number of the substituents in phthalocyanine-sensitized solar cells. Also, their electrochemical and photovoltaic properties were investigated.

2 | EXPERIMENTAL

The used materials, equipment, fabrication, and characterization of DSSCs are supplied in Data S1.

2.1 | Synthesis

2.1.1 | 4-Chloro-5-(3-pyridin-3-ylpropoxy) phthalonitrile (1)

4,5-Dichlorophthalonitrile (0.5 g, 2.5 mmol), 3-(pyridin-3-yl) propan-1-ol (0.8 ml, 5.6 mmol) and dry K_2CO_3 (0.828 g, 5.6 mmol) in anhydrous dimethylformamide (DMF) (15 ml) were stirred under N_2 at 55°C for 2 days. Then, the reaction mixture was poured into water and filtered. The filtrate was extracted with $CHCl_3$:H_2O (60:30) for three times. The organic phase was dried over $MgSO_4$.

The product was purified by column chromatography on aluminum oxide by using $CHCl_3$:MeOH (100:1). Yield: 0.150 g (20%), m.p. 118–120°C. IR (attenuated total reflection [ATR]), ν/cm^{-1}: 3,108 (Ar–H), 2,918–2,849 (Alip. C–H), 2,232 (C≡N), 1,586, 1,548, 1,498, 1,463, 1,421, 1,379, 1,306, 1,271, 1,209, 1,191, 1,130 1,027, 918, 871, 795. ^{1}H-NMR (400 MHz, $CDCl_3$), (δ): 8.50 (s, 2H, Ar–H), 7.81 (s, 1H, Ar–H), 7.57 (d, 1H, Ar–H), 7.25 (m, 1H, Ar–H), 7.22 (s, 1H, Ar–H), 4.14 (t, 2H, –CH_2–O), 2.90 (t, 2H, Ar–CH_2–), 2.26 (q, 2H, –CH_2–). ^{13}C-NMR (100 MHz, $CDCl_3$), (δ): 157.84, 149.92, 147.94, 135.91, 135.70, 134.80, 129.00, 123.56, 116.53, 115.72, 114.79, 114.54, 108.34, 68.76, 29.81, 28.96. Matrix-assisted laser desorption/ionization-time of flight/mass spectrometry (MALDI–TOF–MS) m/z calc. 297.73; found: 298.07 $[M + H]^+$.

2.1.2 | Nonperipherally tetra-3-pyridin-3-ylpropoxy-substituted zinc(II) phthalocyanine (2)

3-(3-Pyridin-3-ylpropoxy)phthalonitrile (**n-Py**) (100 mg, 0.38 mmol), Zn $(CH_3COO)_2$ (37 mg, 0.19 mmol), 1-pentanol (2.5 ml), and 1,8-diazabicyclo[5.4.0]undec-7-ene (DBU) (3 drops) were stirred at 160°C in a sealed glass tube for 24 h under a N_2 atmosphere. The solution was poured into hexane. The precipitate was filtered off, and the product was purified by column chromatography on aluminum oxide by using $CHCl_3$:MeOH (100:1) as solvent system. Yield: 58 mg (36%), m.p. > 300°C. IR (ATR), ν/cm^{-1}: 3,059 (Ar–H), 2,917–2,853 (Alip. C–H), 1,584, 1,486, 1,421, 1,331, 1,264, 1,221, 1,117, 1,108, 1,060, 1,024, 897, 873, 799. ^{1}H-NMR (400 MHz, $CDCl_3$), (δ): 8.97 (s, 4H, Ar–H), 8.68–8.84 (m, 4H, Ar–H), 7.88 (s, 4H, Ar–H), 7.54–7.50 (m, 8H, Ar–H), 6.92–6.88 (m, 8H, Ar–H), 4.46 (bs, 8H, –CH_2–O), 3.18 (bs, 8H, Ar–CH_2–), 2.47–2.43 (m, 8H, –CH_2–). ^{13}C-NMR (100 MHz, $CDCl_3$), (δ): 155.87, 153.65, 153.56, 148.79, 146.41, 141.43, 136.72, 136.39, 130.57, 126.34, 123.37, 115.72, 112.48, 67.82, 29.70, 28.96. UV–Vis (tetrahydrofuran [THF]) λ_{max} nm (log ε): 697 (5.04), 628 (4.35), 362 (4.39), 315 (4.44). MALDI–TOF–MS m/z calc. 1,118.56; found: 1,118.70 $[M]^+$.

2.1.3 | Peripherally tetra-3-pyridin-3-ylpropoxy-substituted zinc(II) phthalocyanine (3)

Zinc(II) phthalocyanine (**3**) was synthesized according to the procedure described for (**2**) by using 4-(3-pyridin-3-ylpropoxy)phthalonitrile. Yield: 55 mg (35%), m.p. > 300°C. IR (ATR), ν/cm^{-1}: 3,028 (Ar–H), 2,917–2,872 (Alip. C–H), 1,604, 1,485, 1,465, 1,421, 1,384, 1,334, 1,274, 1,223, 1,115, 1,087, 1,046, 956, 818, 793. ^{1}H-NMR (400 MHz, $CDCl_3$), (δ): 8.86 (bs, 4H, Ar–H), 8.47–8.43 (m, 8H, Ar–H), 7.57–7.74 (m, 8H, Ar–H), 6.55–6.53 (m, 8H, Ar–H), 4.08–4.04 (m, 8H, –CH_2–O), 2.84–2.85 (m, 8H, Ar–CH_2–), 1.87–1.84 (m, 8H, –CH_2–). ^{13}C-NMR (100 MHz, $CDCl_3$), (δ): 160.84, 150.10, 149.88, 147.56,

141.08, 139.29, 136.76, 136.23, 123.51, 123.43, 118.67, 112.79, 106.24, 67.20, 29.69, 28.95. UV–Vis (THF) λ_{max} nm (log ε): 677 (4.99), 611 (4.34), 350 (4.70). MALDI–TOF–MS m/z calc. 1,118.56; found: 1,118.03 $[M]^+$.

2.1.4 | Peripherally octa-3-pyridin-3-ylpropoxy-substituted zinc(II) phthalocyanine (4)

Zinc(II) phthalocyanine (**4**) was synthesized according to the procedure described for (**2**) by using 4-chloro-5-(3-pyridin-3-ylpropoxy)phthalonitrile. Yield: 35 mg (33%), m.p. > 300°C. IR (ATR), ν/cm^{-1}: 3,027 (Ar–H), 2,918–2,849 (Alip. C–H), 1,602, 1,576, 1,478, 1,436, 1,378, 1,333, 1,256, 1,163, 1,099, 1,065, 1,024, 998, 859, 790. ^{1}H-NMR (400 MHz, $CDCl_3$), (δ): 8.45 (bs, 4H, Ar–H), 8.10 (bs, 4H, Ar–H), 7.54–7.51 (m, 8H, Ar–H), 6.58–6.54 (m, 8H, Ar–H), 4.12–4.09 (m, 8H, $-CH_2-O$), 2.90–2.87 (m, 8H, Ar–CH_2–), 1.94–1.91 (m, 8H, $-CH_2-$). ^{13}C-NMR (100 MHz, $CDCl_3$), (δ): 157.08, 152.98, 150.08, 147.64, 141.05, 139.28, 136.16, 133.43, 130.86, 125.42, 123.46, 113.72, 109.38, 68.34, 29.68, 28.95. UV–Vis (THF) λ_{max} nm (log ε): 676 (5.01), 610 (4.45), 355 (4.82). MALDI–TOF–MS m/z calc. 1,256.34; found: 1,256.68 $[M]^+$.

3 | RESULTS AND DISCUSSION

3.1 | Synthesis and characterization

The synthesis of novel 3-pyridin-3-ylpropoxy-substituted zinc(II) phthalocyanines (**2**, **3**, **4**) is given in Figure 1. 3-(3-(Pyridin-3-yl)propoxy)phthalonitrile (**n-Py**) and 4-(3-(pyridin-3-yl)propoxy)phthalonitrile (**Py**) were synthesized according to the reported procedure.[9,10] 4-Chloro-5-(3-pyridin-3-ylpropoxy)phthalonitrile (**1**) was obtained using conventional method based on aromatic nucleophilic substitution. Zinc(II) phthalocyanines (**2**, **3**, **4**) bearing 3-pyridin-3-ylpropoxy groups were synthesized from the phthalonitrile derivatives (**n-Py**, **Py**, **1**) in 1-pentanol with Zn $(CH_3COO)_2$ and a catalytic amount of DBU.

In the IR spectrum of 4-chloro-5-(3-pyridin-3-ylpropoxy)phthalonitrile (**1**), the appearance of new C≡N vibrations located at 2,232 cm^{-1} supports the formation of the target compound. In the ^{1}H-NMR spectrum of 4-chloro-5-(3-pyridin-3-ylpropoxy)phthalonitrile (**1**), it was observed that new aromatic protons increased compared with those for starting compound.

In the ^{13}C-NMR spectrum, the presence of nitrile carbon atoms was defined, with peaks at δ 115.72 and 114.54 ppm. In the mass spectrum of 4-chloro-5-(3-pyridin-3-ylpropoxy)phthalonitrile (**1**), the $[M + H]^+$ peak at 298.07 verified the suggested structure. In the IR spectra of (**2**, **3**, **4**), sharp –C≡N vibrations of 4-(3-(pyridin-3-yl)propoxy)phthalonitrile, 3-(3-(pyridin-3-yl)propoxy)phthalonitrile, and 4-chloro-5-(3-(pyridin-3-yl)propoxy)phthalonitrile disappeared as expected. The IR spectra of the zinc(II) phthalocyanines (**2**, **3**, **4**) are very similar. The ^{1}H-NMR spectra of the (**2**, **3**, **4**) were recorded in $CDCl_3$. ^{1}H-NMR spectra of (**2**, **3**, **4**) are very similar to those of the starting phthalonitrile derivatives (**n-Py**, **Py**, **1**). In the MALDI–TOF–MS of zinc(II) phthalocyanines (**2**, **3**, **4**), the presence of the molecular ion peaks at m/z = 1,118.70 $[M]^+$ (Figure 2a) for **2**, m/z = 1,118.03 $[M]^+$ (Figure 2b) for **3**, m/z = 1,256.68 $[M]^+$ (Figure 2c) for **4** confirmed the proposed structure. The electronic absorption spectra of 3-pyridin-3-ylpropoxy-substituted zinc(II) phthalocyanines (**2**, **3**, **4**) in THF at room temperature are shown in Figure 3. The UV–Vis spectra (in THF) of the (**2**, **3**, **4**) showed intense absorption peaks (Q band) at 697, 677, and 676 nm, respectively. The other characteristic bands (B bands) were observed at (362, 315), 350, and 355 nm, respectively.

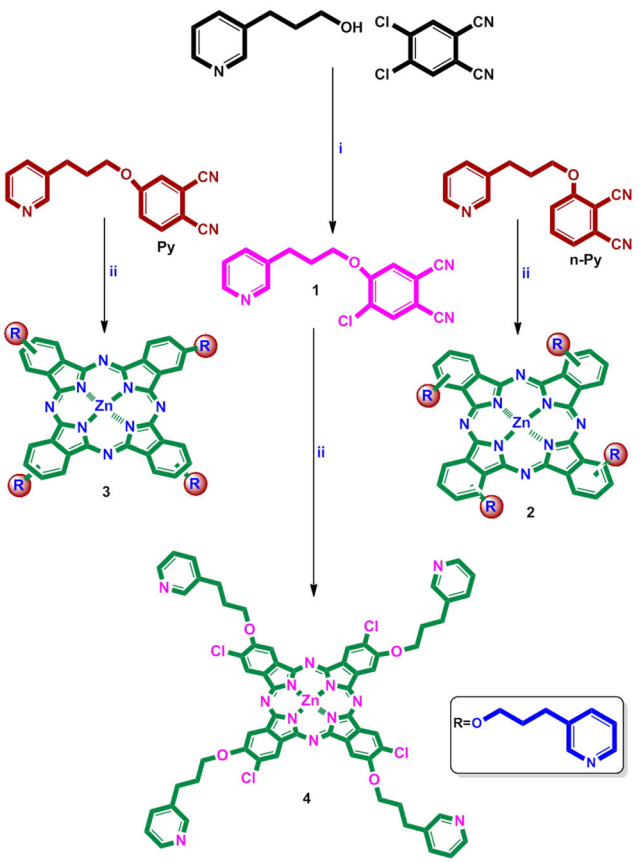

FIGURE 1 The synthesis of novel 3-pyridin-3-ylpropoxy-substituted zinc(II) phthalocyanines (**2**, **3**, **4**). (i) K_2CO_3, 55°C, dimethylformamide (DMF). (ii) Zn $(CH_3COO)_2$, 1-pentanol, 1,8-diazabicyclo[5.4.0]undec-7-ene (DBU), 160°C

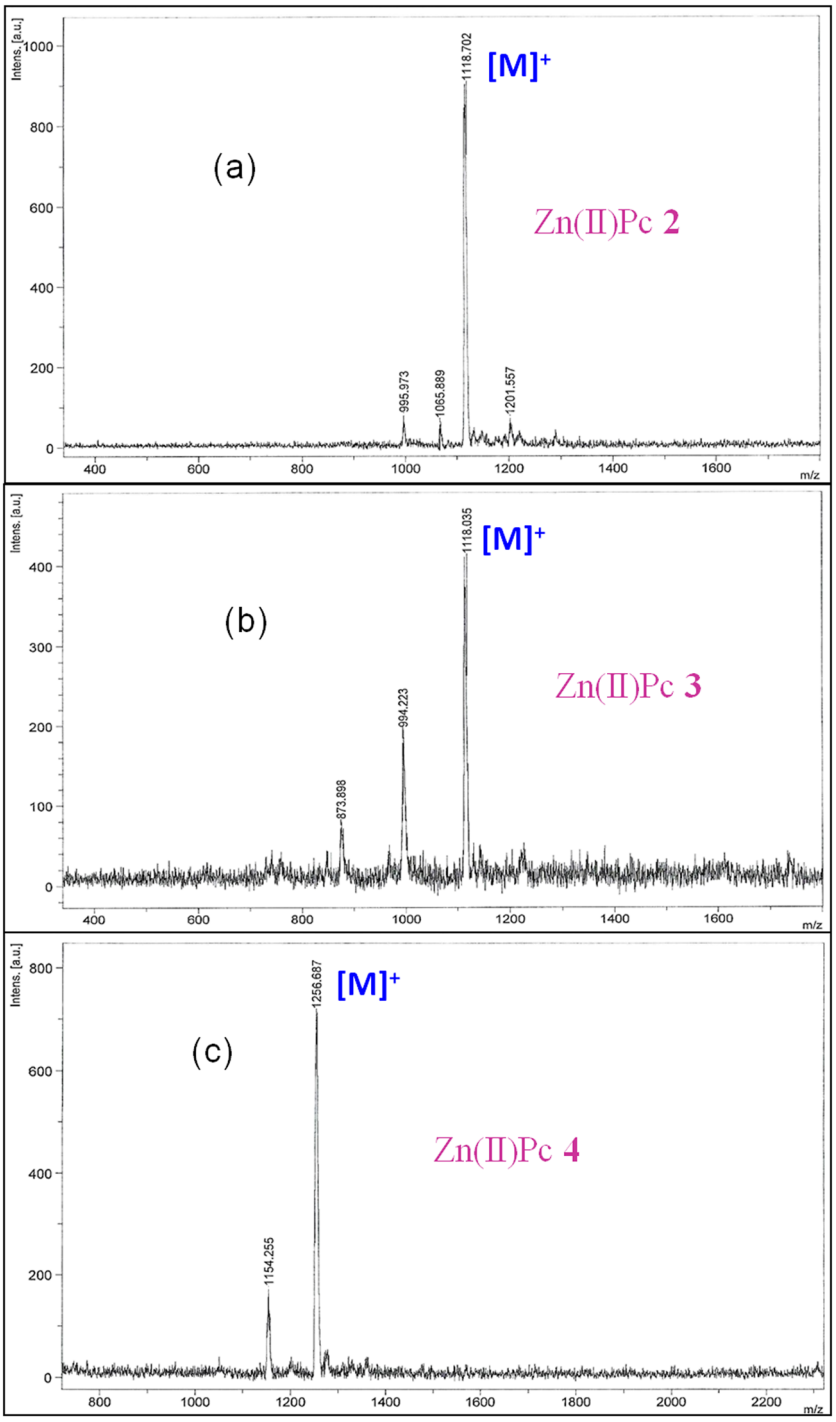

FIGURE 2 (a–c) Matrix-assisted laser desorption/ionization-time of flight/mass spectrometry (MALDI–TOF–MS) of zinc(II) phthalocyanines (**2**, **3**, **4**)

3.2 | Optical properties

The UV–Vis absorption spectra of the three complexes in THF solution and on TiO_2 film are shown in Figure 4, and the corresponding characteristic data are listed in Table 1. As can be seen, the absorption spectra in THF solution exhibit a typical zinc phthalocyanine Q band around 650–700 nm accompanied by a weak vibronic band at around 615–630 nm.[11] The Q band (λ_{max}) of the nonperipheral tetra-substituted complex (**2**) is red-shifted by 20 and 21 nm compared with the peripheral tetra-substituted (**3**) and peripheral octa-substituted (**4**) complexes, respectively. This phenomenon is attributed to the linear combinations of the atomic orbitals (LCAO) coefficients of the HOMO level at the nonperipheral positions that are higher than those at the peripheral positions, resulting in a red shift of the Q band.[12] Compared with the peripheral nonchlorinated complex, the slight blue shift of the λ_{max} for the peripheral chlorinated complex can be ascribed to the electron-withdrawing effect of the

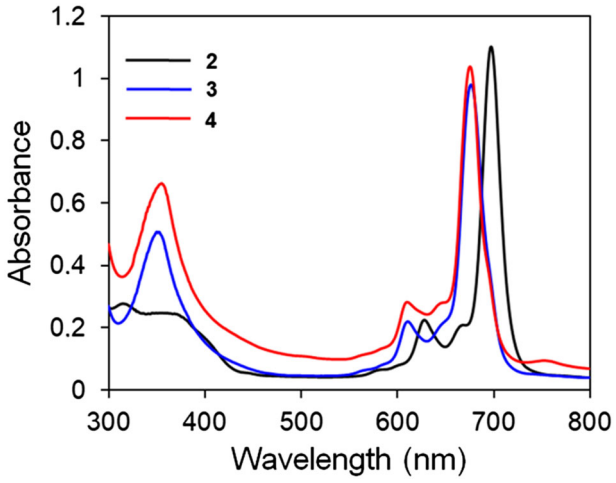

FIGURE 3 UV–Vis spectrum of zinc(II) phthalocyanines (**2**, **3**, **4**) in tetrahydrofuran tetrahydrofuran (THF)

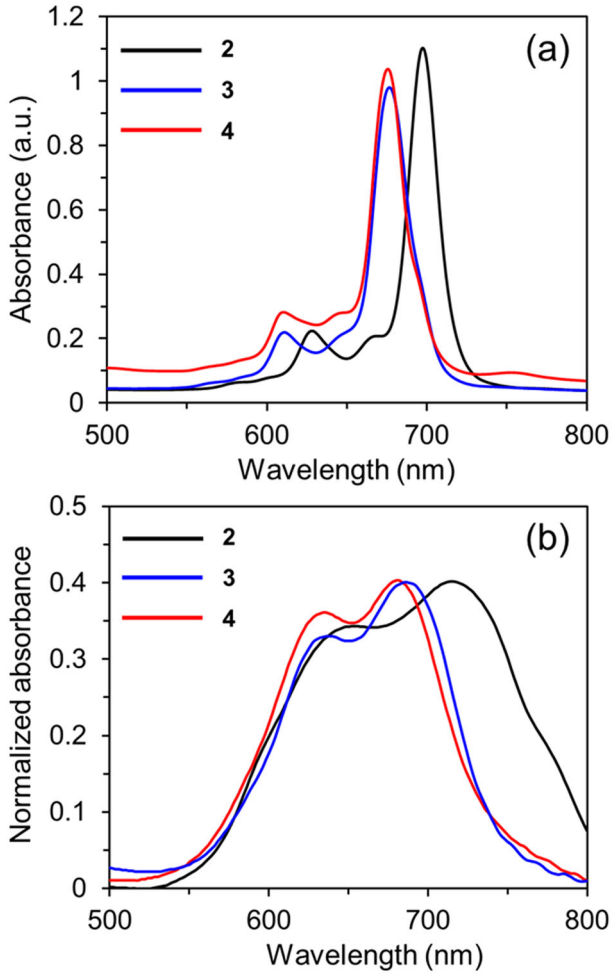

FIGURE 4 Absorption spectra of dyes **2**–**4** (a) in tetrahydrofuran (THF) solution (10^{-5} M) and (b) on TiO_2 film

chlorine atoms, which is consistent with previous studies.[13,14] The spectra of the dyes adsorbed onto TiO_2 film show obviously red-shifted Q bands as well as new bands around 640 nm, indicating the formation of H-aggregates,[15] when compared with the corresponding solution spectra. The red-shifted Q bands might be due to the interaction between the anchoring group of the dye and the TiO_2 surface.[16] This result is consistent with the previous study that the dyes bearing a pyridine electron-withdrawing anchoring group exhibited red-shifted absorption spectra on the TiO_2 films from those in solutions, probably owing to the strong interaction between the pyridine and TiO_2 surface.[17]

3.3 | Electrochemical properties

To evaluate the possibility of the electron injection and regeneration of the three complexes, square wave voltammetry (SWV) experiments were carried out (Figure 5), and the corresponding data were summarized in Table 1. All the complexes exhibited a quasireversible oxidation (O_1) and a quasireversible reduction (R_1), which can be related to the ligand-based redox processes.[18] The HOMO levels of complexes **2**–**4**, calculated from the oxidation potential, are located at 1.03, 1.15, and 1.19 V, respectively. Compared with that of complex **3**, the HOMO level of complex **2** shifts to negative potentials, meaning the latter oxidizes more easily than the former. This shift may be attributed to the stronger electron-donating ability of the nonperipheral position for complex **2**, resulting in a red-shifted absorption spectrum.[19] The HOMO level of complex **4** is slightly more positive than that of complex **3** owing to the electron-withdrawing substituents on the peripheral positions of the former, which leads to a decrease on the electron density thereby leading to more difficult oxidation.[20] It is also shown that the HOMO levels of complexes **2**–**4** are more positive than those of I^-/I_3^- (0.4 V vs. normal hydrogen electrode [NHE]), guaranteeing the efficient dye regeneration.[21] The calculated lowest unoccupied molecular orbital (LUMO) levels of these dyes are more negative than the TiO_2 CB (−0.5 V vs. NHE), ensuring feasible electron injection.[21]

3.4 | Photovoltaic properties of DSSCs

To investigate the photovoltaic performance of DSSCs based on these dyes, the current density–voltage (*J*–*V*) curves of the DSSCs were measured as shown in Figure 6, and the corresponding photovoltaic parameters are summarized in Table 2. Without chenodeoxycholic

TABLE 1 Electro-optical properties of dyes **2**–**4**

Dye	λ_{abs} (nm)[a] (ε [×10^5 M^{-1} cm^{-1}][a])	λ_{onset} (nm)[a]	λ_{abs} (TiO_2) (nm)[b]	E_{0-0} (eV)[c]	HOMO (V)[d]	LUMO (V)[e]
2	697 (1.10)	720	715	1.72	1.03	−0.69
3	677 (0.99)	703	686	1.76	1.15	−0.61
4	676 (1.03)	701	681	1.77	1.19	−0.58

Note. Recorded in THF solutions.

Abbreviations: HOMO, highest occupied molecular orbital; LUMO, lowest unoccupied molecular orbital; NHE, normal hydrogen electrode; THF, tetrahydrofuran.

[a]λ_{abs}, absorption wavelength; ε, molar extinction coefficient; λ_{onset}, absorption onset wavelength.

[b]λ_{abs} (TiO_2): absorption maximum wavelength on the TiO_2 film.

[c]E_{0-0}: band gap, calculated using the equation $E_{0-0} = 1{,}240/\lambda_{onset}$.

[d]HOMO (vs. NHE) was calculated by addition of 0.63 V to the oxidation potential versus Fc/Fc^+.

[e]LUMO (vs. NHE) was obtained by HOMO − E_{0-0}.

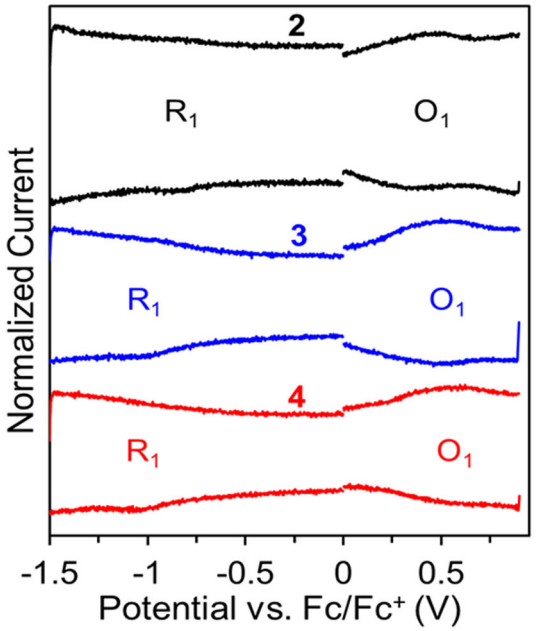

FIGURE 5 Square wave voltammetry (SWV) curves of dyes **2**–**4** on a glassy carbon electrode (GCE) in $TBABF_4$/DMSO

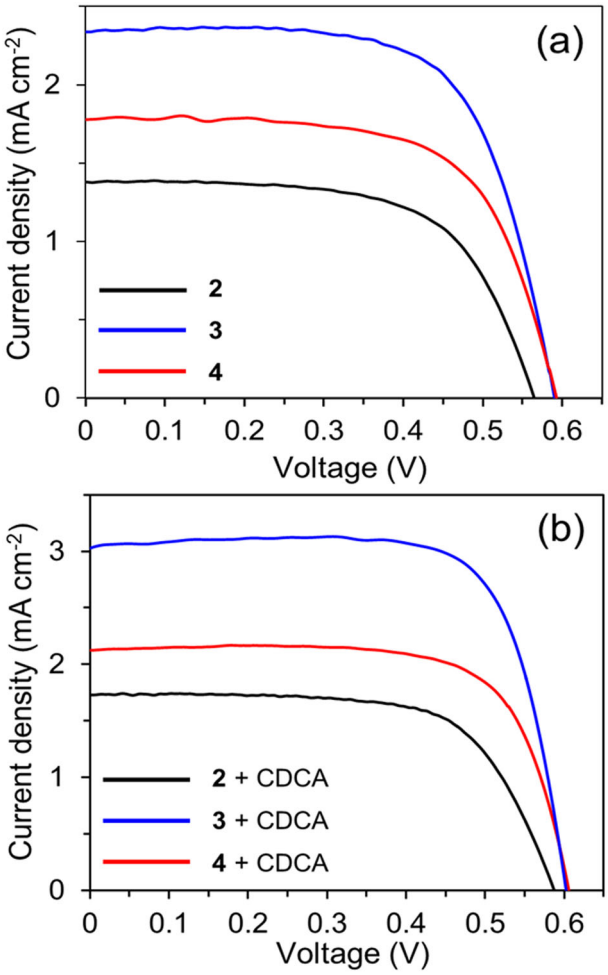

FIGURE 6 *J*–*V* curves of dye-sensitized solar cells (DSSCs) based on dyes **2**–**4**; (a) without and (b) exposed to chenodeoxycholic acid (CDCA)

acid (CDCA), which is a coadsorbent well known to prevent the dye aggregation during the sensitization process, the DSSCs based on complexes **2**–**4** exhibited the short–circuit current density (J_{sc}) in the range of 1.37–2.33 mA cm^{-2}, open–circuit voltage (V_{oc}) in the range of 0.566–0.592 V, and fill factor (FF) in the range of 0.62–0.67, corresponding to PCEs that ranged from 0.48% to 0.93%. As shown in Figure 6a, the PCE of complex **3** is higher than that of complexes **2** and **4** because of the higher J_{sc} and V_{oc}. In the presence of CDCA, the PCE increases in the order of **2** (0.68%) < **4** (0.92%) < **3** (1.36%), which is in parallel with that of the J_{sc} and V_{oc} values (Figure 6b). The PCE and J_{sc} values exhibit in the ranges of 35–46% and 19–29% of enhancement as compared with the solar cells without CDCA, implying that the coadsorbent effectively suppresses the dye aggregation on the TiO_2 surface.[22] Despite the more red-shifted absorption, the photovoltaic performance of the DSSC based on nonperipherally tetra-substituted 3-(pyridin-3-yl)propoxy zinc(II) phthalocyanine sensitizer (**2**) is lower than that of its peripherally substituted

TABLE 2 Photovoltaic parameters of the DSSCs

Dye	J_{sc}^{IPCE} (mA cm^{-2})	J_{SC} (mA cm^{-2})	V_{OC} (V)	FF	PCE (%)	Dye loading amount (mol cm^{-2})
2	1.34	1.37	0.566	0.62	0.48	3.17×10^{-8}
2 + CDCA	1.79	1.73	0.587	0.67	0.68	2.52×10^{-8}
3	2.38	2.33	0.590	0.67	0.93	4.15×10^{-8}
3 + CDCA	3.05	3.01	0.602	0.75	1.36	3.49×10^{-8}
4	1.83	1.79	0.592	0.64	0.68	3.72×10^{-8}
4 + CDCA	2.12	2.13	0.605	0.71	0.92	3.07×10^{-8}
N719 + CDCA	–	14.9	0.780	0.68	7.90	–

Abbreviations: CDCA, chenodeoxycholic acid; DSSC, dye-sensitized solar cell; FF, fill factor; PCE, power conversion efficiency.
[a]J_{sc}^{IPCE} values were integrated from their IPCE spectra.

counterpart (**3**), which may be due to the structural differences among the sensitizers. It is known that the meta-positioned substituents orient the zinc porphyrin with a tilt angle when it binds to the TiO_2 surface, while the para-positioned substituents locate the zinc porphyrin near-orthogonal to the TiO_2 surface.[23] Thus, the meta-positioned units bring the dye closer to the TiO_2 CB and restrict the number of dyes adsorbed onto the TiO_2 surface, which leads to lower PCE.[22] Similarly, as shown in Table 2, the nonperipherally substituted complex (**2**) has the minimum dye loading amount probably due to the largest tilt angle.[24] The lower dye loading amount of complex **2** might provide more free space for the recombination between electrons in the TiO_2 and I_3^- species in the electrolyte, resulting in the lower V_{oc}.[24,25] Complex **2** also could orient with a large tilt angle on the TiO_2 surface owing to the presence of the nonperipheral substituents. Thus, the tilted complex brings the dye closer to the TiO_2 surface, giving a chance to the electrons in the TiO_2 to recombine faster with the dye cations, which leads to lower photocurrent densities.[26] On the other hand, the peripherally substituted dye (**3**) has the highest dye loading amount, which could be related to the vertical orientation of the dye on the TiO_2 surface. It should be noted that the degree of dye coverage was also examined by UV–Vis diffuse reflectance spectroscopy (Figure S1), which is good agreement with the dye loading amounts listed in Table 2. Therefore, complex **3** allows for effective electron injection and inhibits the electron recombination between the injected electrons in the TiO_2 and I_3^- species in the electrolyte,[23,27] resulting in higher J_{sc} and V_{oc}, respectively.

As compared with complex **3**, complex **4** containing extra four chlorine substituents shows slightly higher V_{oc} values with and without CDCA. This can be ascribed to the suppression of recombination between electrons in the TiO_2 and I_3^- species in the electrolyte by incorporating extra substituents around the anchoring groups.[26,28] However, the J_{sc} values for DSSC based on complex **4** are lower than those of complex **3**, which is consistent with less dye loading amounts for the former. The reason for this phenomenon is that the sterically hindered dye structure reduces the adsorption densities of the dye, which decreases the electron injection efficiency, resulting in lower photocurrent densities.[26,29]

The incident photon to current conversion efficiency (IPCE) spectra of the DSSCs based on complexes **2**–**4** with and without CDCA were measured to confirm the trend of J_{sc} variation (Figure 7). In general, the IPCE spectra are consistent with the absorption spectra on the TiO_2 film. The photocurrent responses are in the range of 375–800 nm for complex **2** and 375–775 nm for complexes **3** and **4**, respectively, in the absence of CDCA. Despite that the IPCE spectrum of complex **2** is the broadest, its IPCE intensity in the range of 500–800 nm is the lowest, which is consistent with the lowest J_{sc}. On the other hand, the IPCE values of the DSSC based on complex **3** achieved over 15% from 625 to 750 nm with the highest IPCE value of 18% at 700 nm, indicating the higher J_{sc} value compared with those of complexes **2** and **4**. Note that the integrated IPCE values (J_{sc}^{IPCE}) are in good agreement with the J_{sc} values observed in the J–V tests (Table 2). In the presence of CDCA, the IPCE values of the DSSCs with CDCA are much improved compared with those without CDCA (Figure 7b), which suggests that the coadsorbent suppresses dye aggregation.[30,31]

3.5 | Electrochemical impedance spectroscopy analysis

Electrochemical impedance spectroscopy (EIS) analysis was performed to investigate the electron recombination process in the fabricated DSSCs with CDCA. As shown in Figure 8a, a major semicircle for each DSSC is observed in the Nyquist plots, which corresponds to the middle

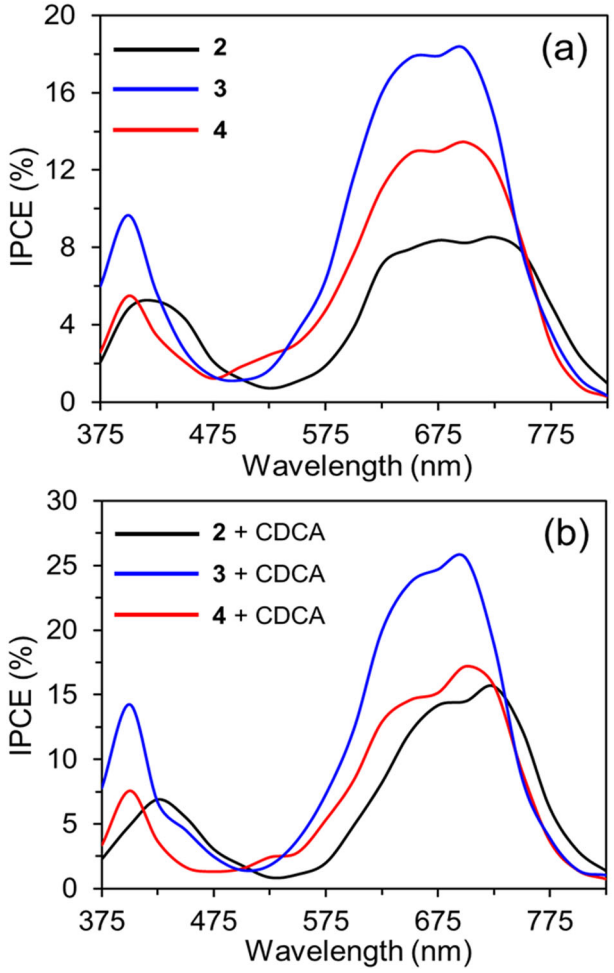

FIGURE 7 IPCE curves of dye-sensitized solar cells (DSSCs) based on dyes **2**–**4**; (a) without and (b) exposed to chenodeoxycholic acid (CDCA)

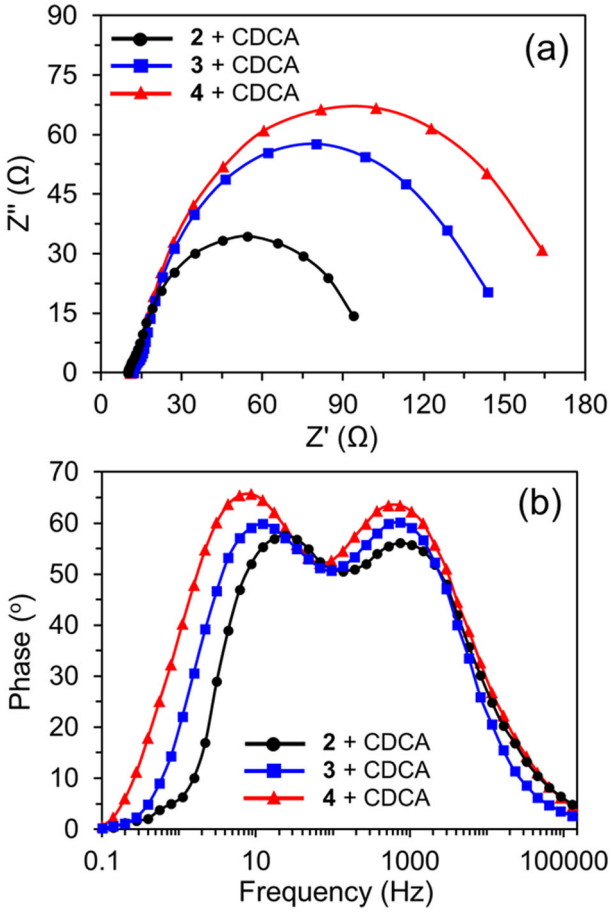

FIGURE 8 (a) Nyquist and (b) Bode plots of dye-sensitized solar cells (DSSCs) based on dyes **2**–**4** with chenodeoxycholic acid (CDCA) in the dark

frequency regions in the Bode plots (Figure 8b), and represents the charge recombination resistance at the TiO_2/dye/electrolyte interface (R_{rec}). A larger radius of the major semicircle means slower electron recombination between electrons in the TiO_2 and the redox electrolyte and therefore a higher photovoltage.[32] As shown in Figure 8a, the radius of the R_{rec} increases in the order of **2** (78 Ω) < **3** (119 Ω) < **4** (132 Ω). The electron lifetimes of **2**–**4** are found to be 6.6, 12.3, and 18.4 ms, respectively (Figure 8b). Consequently, the larger R_{rec} and longer electron lifetime may be the main reason for the higher photovoltage of complex **4**.

4 | CONCLUSIONS

In summary, novel 3-pyridin-3-ylpropoxy-substituted zinc(II) phthalocyanines (**2**, **3**, **4**) were synthesized and used as sensitizers in DSSCs. The photophysical and electrochemical studies indicated that all the phthalocyanines were capable of serving as sensitizers for DSSCs. The DSSC based on complex **3** shows not only enhanced electron injection but also decreased electron recombination, which could be related to the vertical orientation of the dye on the TiO_2 surface. As a result, the DSSC based on **3** exhibits the highest PCE of 1.36% with the J_{sc}, V_{oc}, and FF values of 3.01 mA cm^{-2}, 0.602 V, and 0.75, respectively, in the presence of the coadsorbent. The results indicate that incorporating peripheral substituted 3-(pyridin-3-yl)propoxy as an anchoring group to zinc(II) phthalocyanines can enhance the PCE.

ACKNOWLEDGEMENT

This study was not supported by any organization.

AUTHOR CONTRIBUTIONS

Turgut Keleş: Methodology. **Zekeriya Bıyıklıoğlu:** Formal analysis; funding acquisition; investigation; methodology; supervision. **Emre Güzel:** Investigation;

methodology. **Mehmet Nebioğlu:** Methodology. **İlkay Şişman:** Investigation; methodology.

Data Availability Statement

The data that support the findings of this study are available from the corresponding author upon reasonable request.

ORCID

Zekeriya Biyiklioglu https://orcid.org/0000-0001-5138-214X
Emre Güzel https://orcid.org/0000-0002-1142-3936
Mehmet Nebioğlu https://orcid.org/0000-0002-2603-3906
İlkay Şişman https://orcid.org/0000-0002-0943-2817

REFERENCES

[1] M. Urbani, M. E. Ragoussi, M. K. Nazeeruddin, T. Torres, *Coord. Chem. Rev.* **2019**, *381*, 1.
[2] C. C. Raj, R. Prasanth, *J. Power Sources* **2016**, *317*, 120.
[3] I. López-Duarte, M. Wang, R. Humphry-Baker, M. Ince, M. V. Martínez-Díaz, M. K. Nazeeruddin, T. Torres, M. Grätzel, *Angew. Chemie* **2012**, *124*, 1931.
[4] D. Çakir, T. Arslan, Z. Biyiklioglu, *Dalton Trans.* **2015**, *44*, 20859.
[5] E. Güzel, A. Koca, A. Gül, M. B. Koçak, *Synth. Met.* **2015**, *199*, 372.
[6] M. K. Nazeeruddin, R. Humphry-Baker, D. L. Officer, W. M. Campbell, A. K. Burrell, M. Grätzel, *Langmuir* **2004**, *20*, 6514.
[7] E. Güzel, İ. Şişman, A. Gül, M. B. Koçak, *J. Porphyr. Phthalocyanines* **2019**, *23*, 279.
[8] L. Zhang, J. M. Cole, *ACS Appl. Mater. Interfaces* **2015**, *7*, 3427.
[9] T. Keleş, B. Barut, Z. Biyiklioglu, A. Özel, *Dyes Pigm.* **2017**, *139*, 575.
[10] T. Krivica, M. Roze, N. Kiricenko, V. Kampars, *Mater. Sci. Appl. Chem.* **2013**, *27*, 50.
[11] J. Y. Liu, P. C. Lo, X. J. Jiang, W. P. Fong, D. K. P. Ng, *Dalton Trans.* **2009**, *2009*, 4129.
[12] P. Mashazi, E. Antunes, T. Nyokong, *J. Porphyr. Phthalocyanines* **2010**, *14*, 932.
[13] S. Wei, D. Huang, L. Li, Q. Meng, *Dyes Pigm.* **2003**, *56*, 1.
[14] T. Kimura, H. Muraoka, S. Nakajo, S. Ogawa, S. Yamamoto, N. Kobayashi, *European J. Org. Chem.* **2018**, *2018*, 1255.
[15] J. He, G. Benkö, F. Korodi, T. Polívka, R. Lomoth, B. Åkermark, L. Sun, A. Hagfeldt, V. Sundström, *J. Am. Chem. Soc.* **2002**, *124*, 4922.
[16] P. V. Kamat, *Chem. Rev.* **1993**, *93*, 267.
[17] Y. Ooyama, S. Inoue, T. Nagano, K. Kushimoto, J. Ohshita, I. Imae, K. Komaguchi, Y. Harima, *Angew. Chem., Int. Ed.* **2011**, *50*, 7429.
[18] Z. Biyiklioğlu, V. Çakir, D. Çakir, H. Kantekin, *J. Organomet. Chem.* **2014**, *749*, 18.
[19] S. Z. Topal, Ü. Işci, U. Kumru, D. Atilla, A. G. Gürek, C. Hirel, M. Durmuş, J. B. Tommasino, D. Luneau, S. Berber, F. Dumoulin, V. Ahsen, *Dalton Trans.* **2014**, *43*, 6897.
[20] Z. Zhao, K. I. Ozoemena, D. M. Maree, T. Nyokong, Dalt. Trans. **2005**, 1241–1248.
[21] F. Lu, J. Zhang, Y. Zhou, Y. Zhao, B. Zhang, Y. Feng, *Dyes Pigm.* **2016**, *125*, 116.
[22] J. S. Ni, W. S. Kao, H. J. Chou, J. T. Lin, *ChemSusChem* **2015**, *8*, 2932.
[23] R. B. Ambre, S. B. Mane, G. F. Chang, C. H. Hung, *ACS Appl. Mater. Interfaces* **2015**, *7*, 1879.
[24] H. Ellis, S. K. Eriksson, S. M. Feldt, E. Gabrielsson, P. W. Lohse, R. Lindblad, L. Sun, H. Rensmo, G. Boschloo, A. Hagfeldt, *J. Phys. Chem. C* **2013**, *117*, 21029.
[25] T. Ripolles-Sanchis, B. C. Guo, H. P. Wu, T. Y. Pan, H. W. Lee, S. R. Raga, F. Fabregat-Santiago, J. Bisquert, C. Y. Yeh, E. W. G. Diau, *Chem. Commun.* **2012**, *48*, 4368.
[26] B. G. Kim, K. Chung, J. Kim, *Chem. - A Eur. J.* **2013**, *19*, 5220.
[27] H. Zhou, J. M. Ji, S. H. Kang, M. S. Kim, H. S. Lee, C. H. Kim, H. K. Kim, *J. Mater. Chem. C* **2019**, *7*, 2843.
[28] Y. Hua, L. T. Lin Lee, C. Zhang, J. Zhao, T. Chen, W. Y. Wong, W. K. Wong, X. Zhu, *J. Mater. Chem. A* **2015**, *3*, 13848.
[29] L. Tejerina, M. V. Martínez-Díaz, M. K. Nazeeruddin, M. Grätzel, T. Torres, *ChemPlusChem* **2017**, *82*, 132.
[30] B. Yıldız, E. Güzel, D. Akyüz, B. S. Arslan, A. Koca, M. K. Şener, *Sol. Energy* **2019**, *191*, 654.
[31] B. S. Arslan, E. Güzel, T. Kaya, V. Durmaz, M. Keskin, D. Avcı, M. Nebioğlu, İ. Şişman, *Dyes Pigm.* **2019**, *164*, 188.
[32] X. Qian, L. Lu, Y. Z. Zhu, H. H. Gao, J. Y. Zheng, *RSC Adv.* **2016**, *6*, 9057.

SUPPORTING INFORMATION

Additional supporting information may be found online in the Supporting Information section at the end of this article.

How to cite this article: Keleş T, Biyiklioglu Z, Güzel E, Nebioğlu M, Şişman İ. Dye-sensitized solar cells based on zinc(II) phthalocyanines bearing 3-pyridin-3-ylpropoxy anchoring groups. *Appl Organomet Chem*. 2020;e6076. https://doi.org/10.1002/aoc.6076